Kinetics and Mechanism of the Citrate Synthase from the Thermophilic Archaeon *Thermoplasma acidophilum*†

Linda C. Kurz,*,‡ George Drysdale,‡ Marian Riley,‡ Maharaj Alejandro Tomar,‡ Judy Chen,‡ Rupert J. M. Russell,§ and Michael J. Danson§

Department of Biochemistry and Molecular Biophysics, Division of Biology and Biomedical Sciences, Washington University School of Medicine, St. Louis, Missouri 63110, and Centre for Extremophile Research, Department of Biology and Biochemistry, University of Bath, Bath BA2 7AY, U.K.

Received August 24, 1999; Revised Manuscript Received December 8, 1999

ABSTRACT: The kinetics and mechanism of the citrate synthase from a moderate thermophile, *Thermoplasma acidophilum* (TpCS), are compared with those of the citrate synthase from a mesophile, pig heart (PCS). All discrete steps in the mechanistic sequence of PCS can be identified in TpCS. The catalytic strategies identified in PCS, destabilization of the oxaloacetate substrate carbonyl and stabilization of the reactive species, acetyl-CoA enolate, are present in TpCS. Conformational changes, which allow the enzyme to efficiently catalyze both condensation of acetyl-CoA thioester and subsequently hydrolysis of citryl-CoA thioester within the same active site, occur in both enzymes. However, significant differences exist between the two enzymes. PCS is a characteristically efficient enzyme: no internal step is clearly rate-limiting and the condensation step is readily reversible. TpCS is a less efficient catalyst. Over a broad temperature range, inadequate stabilization of the transition state for citryl-CoA hydrolysis renders this step nearly rate-limiting for the forward reaction of TpCS. Further, excessive stabilization of the citryl-CoA intermediate renders the condensation step nearly irreversible. Values of substrate and solvent deuterium isotope effects are consistent with the kinetic model. Near its temperature optimum (70 °C), there is a modest increase in the reversibility of the condensation step for TpCS, but reversibility still falls short of that shown by PCS at 37 °C. The root cause of the catalytic inefficiency of TpCS may lie in the lack of protein flexibility imposed by the requirement for thermal stability of the protein itself or its temperature-labile substrate, oxaloacetate.

Citrate synthase catalyzes a Claisen condensation between the carbonyl of oxaloacetate (OAA)[1] and the acetyl methyl of the thioester, acetyl-coenzyme A (AcCoA). This enzyme is critical to the energy-yielding and biosynthetic pathways of a wide range of organisms from psychrophiles (*13*) to hyperthermophiles (*14*). Consequently, the catalytic machinery has been optimized for a corresponding wide range of environmental temperatures. A detailed dissection of the kinetics and mechanisms of enzymes isolated from evolutionarily distant organisms thriving in diverse environments may be expected to reveal what catalytic strategies are essential as well as how they may be fine-tuned to accommodate large differences in environmental temperature.

Citrate synthase is particularly appropriate for such comparative studies. It is a prototype system, illustrating several of the important issues in mechanistic enzymology. Citrate synthases use substrate destabilization to increase reactivity (OAA carbonyl polarization) while stabilizing a reactive nucleophile, AcCoA enolate, resulting from proton transfer from a carbon acid (methyl group of AcCoA) possibly via a strong, short hydrogen bond. There is evidence for the functioning of catalytic residues in unusual ionization states (possible imidazolate intermediates at H274 and H320). Changes in macromolecular conformation and protein flexibility are necessary components of the catalytic machine. A great deal of structural (*15*), kinetic (*16*−*19*), and mechanistic information (*5*) is available for the mesophile enzyme from pig heart (PCS). Structural and preliminary kinetic data are available for several extremophile enzymes (*13, 14*). This report is the first in a series in which we will examine in depth the mechanism of citrate synthases isolated from various extremophiles.

The citrate synthase (TpCS) originates in a thermophilic archaeon, *Thermoplasma acidophilum*, which grows at 55−60 °C, pH 1−2. The primary sequence homology with PCS is low, 20% (*20*). However, the active sites of the two enzymes display almost identical composition and conformation. The three main catalytic residues and several substrate binding residues, as well as a number of residues near the active site whose roles have not yet been identified, are either

† Supported by National Institutes of Health Grant GM33851 (L.C.K.) and the Biotechnological and Biological Science Research Council, U.K. (M.J.D. and R.J.M.R.). Support for M.J.T. was provided in part by a grant to Washington University from the Howard Hughes Medical Institute through the Undergraduate Biological Sciences Education Program.

‡ Washington University School of Medicine.

§ University of Bath.

[1] Abbreviations: AcCoA, acetyl-coenzyme A; CD, circular dichroism; CitCoA, *S*-citryl-coenzyme A; PCS, citrate synthase from pig heart; DTNB, 5,5′-dithiobis(2-nitrobenzoic acid); OAA, oxaloacetate; CM-CoA, carboxymethyl-coenzyme A; CMX, carboxymethyldethia-coenzyme A; dethiaAcCoA, dethiaacetyl-coenzyme A; cMDH, cytoplasmic malate dehydrogenase from pig heart; PfCS, citrate synthase from *Pyrococcus furiosus*; SAS, saturated ammonium sulfate solution; TMDH, malate dehydrogenase from *Thermus aquaticus;* TIM, triosephosphate isomerase; TpCS, citrate synthase from *Thermoplasma acidophilum*.

10.1021/bi991982r CCC: $19.00
Published on Web 02/12/2000

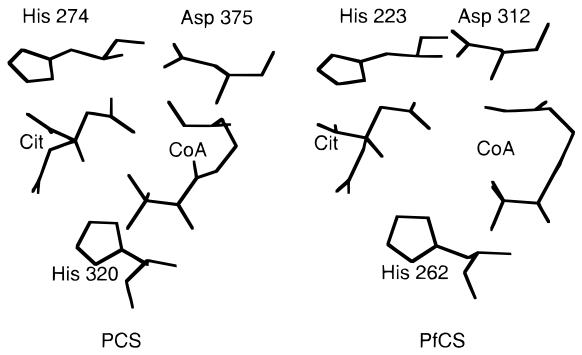

FIGURE 1: Active-site similarities. Citrate-CoA complexes of citrate synthases from pig heart (*21*) and from *Pyrococcus furiosus* (*14*) are shown.

identical or conservative replacements. In addition, several residues (which may be involved in obligate conformational changes) are also retained in the domain interface and elsewhere. While all 16 helices of TpCS have their counterparts in PCS, TpCS is a more compact protein than PCS. The loops connecting elements of secondary structure are shorter in TpCS and it is missing four surface-accessible helices found in PCS. Both proteins are homodimers. Each subunit has a large and a small domain. The active site contains residues from the large domain of one subunit and the small domain of the other.

The X-ray structures of citrate synthases fall into two general conformational classes, open and closed forms. Open and closed refer to the accessibility of the active site to bulk solvent. The open conformation is believed to allow association of substrates and dissociation of products. All chemical transformations, including both condensation and hydrolysis, are believed to take place in closed forms in which the active site is buried deep within the protein. While the only X-ray structure available for TpCS is in the open conformation, solution studies (NMR, CD) of various ternary complexes (vide infra) have unmistakable spectroscopic signatures of the closed forms. Figure 1A shows the active site of one of the closed forms of PCS, the citrate-CoA ternary complex (*21*), and Figure 1B shows the active site of the closed form of the corresponding citrate-CoA complex of PfCS, a related archaeal enzyme isolated from *Pyrococcus furiosis* (*14*).

The broad outlines of the catalytic strategies of the two enzymes are similar even in the absence of extensive primary sequence identity, perhaps as a consequence of similarities in local active site structures and overall secondary, tertiary, and quaternary structures. All the discrete steps in the mechanistic sequence of PCS can be identified in TpCS. Both enzymes polarize the carbonyl of oxaloacetate, enhancing its reactivity toward an acetyl-CoA carbon nucleophile, acetyl-CoA enolate. To generate the enolate, they catalyze proton transfer from the acetyl-CoA methyl group to an active-site Asp. The overall reaction proceeds in two steps with a stable intermediate, citryl-CoA, as the immediate product of the condensation reaction. This tightly bound chemical intermediate is then hydrolyzed to the eventual products, citrate and CoA, within the same active site. Conformational changes between open and several closed forms accompany the binding of oxaloacetate, the formation of the ternary complexes, and the switch from catalysis of condensation to catalysis of hydrolysis. However, differences do exist. Notable is the lower catalytic efficiency of TpCS. Even at 70 °C, the k_{cat} for TpCS is still only 5200 min^{-1} compared to 21 000 min^{-1} for PCS at 37 °C. The lower k_{cat} is offset slightly by tighter substrate binding to TpCS. The cause of this lower catalytic efficiency may lie in suboptimal internal thermodynamics (as explained in ref *22*). Efficient enzymes have no step overwhelmingly rate-determining. Their internal equilibria are readily reversible with equilibrium constants substantially closer to 1.0 than are those of the corresponding free solution reaction. Unlike PCS, TpCS has the hydrolysis step nearly rate-determining over a wide range of pH's and temperatures. Furthermore in contrast to PCS, the condensation step for TpCS is practically irreversible. While the catalytic efficiency improves at the environmental temperature of the source organism, it falls short of that for PCS. Catalytic efficiency may be compromised by the requirement for thermal stability of the protein itself or its temperature-labile substrate, OAA.

MATERIALS AND METHODS

Enzymes.[2] Crystalline citrate synthase from pig heart (PCS) was obtained from Sigma Chemical Co., St. Louis, MO.

Citrate Synthase from Thermoplasma acidophilum (TpCS). The citrate synthase gene from *T. acidophilum* in plasmid pCSEH19 (*23*) was recloned into expression vector pRec7-NdeI (M. Bittner), an *Nde*I site-containing version of pARC306A (*24*) having a consensus sequence synthetic RecA promoter and T7 translation enhancer. The gene was cloned via *Ase*I sites at either end into the compatible *Nde*I site of the vector, such that the ribosome-binding site of the vector was retained but translation would initiate at the normal start codon of the TpCS gene. The correct construct was confirmed by restriction analysis and sequencing of the resultant plasmid DNA (named pRec7-ArCS).

The preparation of TpCS from *Escherichia coli* strain MG1655 transformed with pRec7-ArCS generally follows the procedures of ref *25* with some modifications. After the heat treatment, the supernatant solution is made 0.25% (w/v) with neutralized poly(ethylenimine) to remove polynucleotides. Some protein impurities are removed by precipitation by bringing the solution to 50% SAS. The TpCS is precipitated at 85% SAS and stored at 4 °C until affinity chromatography on Dyematrex Gel Red A (Millipore Corp.). After dialysis against buffer (20 mM Tris and 1 mM EDTA, pH 8.0), the enzyme activity is absorbed on a minimum amount of the resin, which is then packed into a column containing an additional 10% resin. After washing the column with loading buffer, the enzyme is eluted with a linear salt gradient from 0 to 0.5 M NaCl in loading buffer. The active fractions are pooled, concentrated to 5−10 mg mL^{-1} using a Centricon 20 centrifuge concentrator (Amicon Corp.), and then precipitated with 85% SAS for storage. The enzyme is at least 95% pure by SDS−polyacrylamide gel electrophoresis (data not shown).

Isoelectric focusing experiments under native conditions were run in precast agarose gels, pH range 3−10 (FMC Corp.). A broad range p*I* standard (Pharmacia Corp) was run adjacent to lanes containing protein samples. Electrophoresis under native conditions on 1% agarose gels was

[2] Enzyme concentrations are given in terms of active sites (not the dimer).

run in 25 mM Tris buffer, pH 8.0. To detect migration in either direction, samples were loaded in the middle of the gel.

Substrates and Inhibitors. [2-^{13}C]-OAA was prepared as described in ref *26*; CMCoA and [1-^{13}C]-CMCoA according to ref *27* with modifications as described previously (*26*); and CitCoA as in ref *28*. For experiments that required CitCoA in D_2O, the final G-10 desalting column was run in 1 mM DCl. Dethiaacetyl-CoA was obtained from Dr. Dale Drueckhammer, who prepared it according to ref *29*. CD_3-AcCOA was prepared by the reaction of acetic anhydride-d_6 with an excess of CoA according to ref *30* and purified according to ref *31*.

Kinetic Methods and Substrate Concentrations. Absorbance data were collected on a Cary 3 spectrophotometer. Temperature of solutions was controlled to ±0.1 °C. Concentrations of AcCoA, OAA, and CitCoA were measured enzymatically with PCS or TpCS. CoA concentrations were measured by a DTNB assay (*32*). Citrate synthase activity (*33*) with the normal substrates, OAA and AcCoA, was monitored through the reaction of the sulfhydryl product, CoA, with DTNB, producing TNB, which absorbs at 412 nm (ϵ = 14.1 mM^{-1}; *32*). Alternatively, AcCoA−OAA disappearance was monitored by the absorbance change at 233 nm ($\Delta\epsilon$ = 5.4 mM^{-1}; *34*), which is dominated by the thioester absorbance. With CitCoA as substrate, three different assays have been employed as indicated in the description of individual experiments. The concentrations of thioesters (AcCoA/CitCoA) are monitored directly through the characteristic absorption at 236 nm ($\Delta\epsilon$ = −4.96 mM^{-1}; *28*). CoA produced from hydrolysis is monitored at 412 nm ($\Delta\epsilon$ = 14.1 mM^{-1}) through reaction of its sulfhydryl with the thiol reagent DTNB (*32*). OAA produced from cleavage of CitCoA is reduced to malate by cMDH with concomitant oxidation of NADH ($\Delta\epsilon$ = −6.22 mM^{-1}). At temperatures above 35 °C, the thermostable MDH from *Thermus aquaticus* (Sigma Chemical Co.) was used for the same purpose. No significant temperature or pH dependence was found for thioester (AcCoA and CitCoA) and NADH extinction coefficients. The pH values of reaction mixtures were measured in the cuvettes after the reactions had gone to completion by use of a microcombination pH electrode (model MI-412, Microelectrodes, Inc.) with a 2-point calibration against pH standard buffers at the temperature of the experiment.

Circular Dichroism. Spectra and titration data were collected and analyzed as previously described (*26*).

Fluorescence. Spectra and titration data were obtained on a PTI Alpha scan spectrofluorometer with a thermostatted cell compartment. Excitation and emission wavelengths and other instrument parameters are included in Results where appropriate.

Carbon-13 NMR. C-13 spectra were obtained at 150.7 MHz on a Varian Unity 600 spectrometer or at 125.7 MHz on a Varian VXR-500 spectrometer, both equipped with a 5-mm multinuclear probe. Proton-decoupled spectra were obtained by Waltz decoupling. The sample buffer was 50 mM Tris-HCl and 1 mM EDTA, "pH" = 7.50, and included 25% D_2O (for internal lock) and 0.15 M acetonitrile (as internal chemical shift standard). Samples were thermostatted at various temperatures as indicated in Results. Other details were as described previously (*26*).

Proton NMR. Proton spectra were obtained at 500 MHz on a Varian Unity-Plus 500 spectrometer equipped with a 5-mm reverse probe (Nalorac, Martinez, CA). Residual water signals were suppressed by transmitter presaturation (continuous wave decoupling centered on the water frequency) during the delay between acquisitions. Spectra were collected at 25 °C with a 90° pulse, and the delay between acquisitions was set to at least 5 times the T_1 value of the slowest relaxing proton of interest. Conditions were similar to those described in ref *5*.

Solvent Exchange of the Methyl Protons of DethiaAcCoA and AcCoA. Enzyme samples for all exchange experiments were exchanged into the D_2O buffer for the experiment. Data were collected and analyzed as previously described for PCS and its mutants (*24*).

Solvent Exchange into the Methylene of Citrate with AcCoA and CitCoA as Substrates. The exchange of solvent deuterons into the methylene of citrate starting with either AcCoA or CitCoA was done as in the exchange experiments reported for PCS (*5*). Data for CitCoA were collected under two conditions, OAA release reversible and OAA release irreversible. In all cases, the *overall* reaction, net citrate production, was made irreversible by including DTNB in the reaction mixture. The first condition (OAA release reversible) has only DTNB trapping so that any OAA released by CitCoA cleavage also eventually ends up as citrate. The second type of experiment (OAA release irreversible) includes cMDH and NADH to capture and reduce any OAA released after cleavage of CitCoA. The incorporation of deuterium into citrate isolated from reactions was determined by mass spectrometry as described previously (*5*).

RESULTS

Preparation and Additional Properties of TpCS. Recloning of the gene into a high-yield expression system was required because of the large amounts of protein needed for NMR experiments. The correct construct was identified by rescue of a GltA$^-$ strain for growth on acetate. Further confirmation was obtained by isolation of an enzyme having heat-resistant citrate synthase activity, the expected size (42 941 Da by electrospray mass spectrometry), and the expected N-terminal amino acid sequence (electrospray and sequencing data not shown). Synthesis of recombinant protein in this system is induced with nalidixic acid and yields 150−200 mg of enzyme/L of culture in rich medium.

Isoelectric Point (data not shown). Plots of p*I* of standard proteins vs distance from the cathode were linear and the p*I* of the native TpCS is found to be 8.9. The calculated p*I* based on the composition (and confirmed under denaturing conditions) is 8.0. It is clear that one or more of the residues in this protein has an unusual pK_a. When loaded on a native gel at pH 8.0, TpCS and its complexes are found to migrate toward the cathode, while PCS and its complexes migrate in the opposite direction toward the anode.

Near-UV (250−300 nm) CD Spectra of Free Enzymes and Binary and Ternary Complexes. The near UV (λ > 250 nm) CD spectra of proteins arise from induced CD in the chromophores of the aromatic amino acids. The specific positions of chromophore side chains relative to the chiral peptide backbone are the origins of these signals, and changes in them are sensitive monitors of conformational changes. An induced CD signal is also frequently observed for

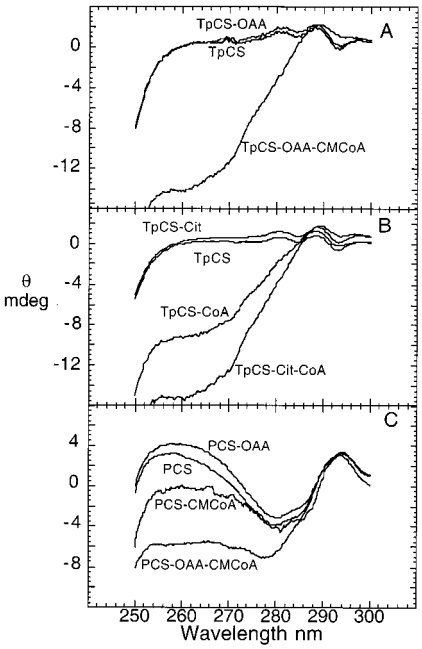

FIGURE 2: Near-UV CD spectra of PCS, TpCS, and some of their complexes. (A) From the top: TpCS−OAA (15 μM TpCS and 100 μM OAA, 1 cm path length), TpCS (15 μM, 1 cm path length), TpCS−OAA−CMCoA (15 μM TpCS, 100 μM OAA, and 50 μM CMCoA, 1 cm path length, excess CMCoA subtracted). (B) From the top: TpCS−Cit (15 μM TpCS and 40 mM citrate, 1 cm path length), TpCS (15 μM, 1 cm path length) TpCS−CoA (150 μM TpCS and 1 mM CoA, 0.1 cm path length, excess CoA subtracted), TpCS−Cit−CoA (150 μM TpCS, 40 mM citrate, and 1 mM CoA, 0.1 cm path length, excess CoA subtracted). (C) From the top: PCS−OAA (15 μM PCS and 100 μM OAA, 1 cm path length), PCS (15 μM PCS, 1 cm path length), PCS−CMCoA (150 μM PCS and 1 mM CMCoA, 0.1 cm path length, excess CMCoA subtracted), PCS−OAA−CMCoA (15 μM PCS, 100 μM OAA, and 50 μM CMCoA, 1 cm path length, excess CMCoA subtracted).

complexes of enzymes with ligands whose chromophores absorb in this region.

The spectra for the free enzymes and various binary and ternary complexes are shown in Figure 2.

The CD changes that accompany formation of complexes with CS are large enough to be quantitatively useful. The stoichiometric (active-site) titration of TpCS−OAA (prepared from a stock of known 280 absorbance) with the intermediate analogue, CMCoA, was used to measure the TpCS 280 nm extinction coefficient. We obtained a value of 1.43 OD_{280} mL mg^{-1}. At lower enzyme concentrations, these CD changes accompanying formation of ternary and binary complexes are used to determine ligand dissociation constants (*24*, *26*) as shown in Table 1. The wavelength of maximum change was used for these titrations.

The differences between the spectra of the free enzymes reflect their differences in amino acid compositions. The changes in the CD spectra of the enzymes that accompany OAA or citrate binding are a result of conformational changes in the enzymes since citrate and the keto form of OAA (which is the form that binds to CS; *34*−*36*) have no chromophore in this spectral region. Much of the large change near 260 nm in the CD spectra of ternary complexes with CoA analogues (AcCoA, dethiaAcCoA, CMCoA, and CoA) (*24*) may be attributed to induced CD from the strong immobilization of the coenzyme's adenine chromophore against the chiral enzyme surface.

Table 1: Ligand Dissociation Constants[a] for PCS and TpCS at 20 °C

complex	OAA (μM)	AcCoA (μM)	dethiaAcCoA (μM)	CoA (μM)	citrate (μM)	CMCoA (μM)
TpCS	0.86[b]	26[c]	nd	16[c]	108[d]	nd
PCS	4[e]	64[c] 147[f]	nd	111[f]	nd	52[c]
TpCS−OAA			1.6[c]	nd		0.043[c]
PCS−OAA		5[f]	2.3[c,g]	14[c]		0.023[c,h]
TpCS−CoA	nd				?	
PCS−CoA	nd				500[f]	
TpCS−citrate		nd	nd	20[c]		nd
PCS−citrate		nd	nd	59[c]		nd

[a] Uncertainties (standard deviation) range from 5% to 10% of the value. [b] Determined by fluorescence titration exciting at 290 nm with emission measured at 315 nm. [c] Determined by CD titration at 260 nm. [d] Determined by CD titration at 280 nm. [e] Reference 70. [f] Determined by competition with a bound spin-labeled analogue of AcCoA or by effects of addition of second ligand on dissociation of the spin-labeled analogue (*71*). [g] Reference 24. [h] Reference 26.

The shapes and amplitudes of the spectra of CoA analogue complexes reveal some qualitative and quantitative differences between the enzymes (Figure 2). Both ternary and binary TpCS complexes have larger amplitudes than the corresponding PCS complexes. The binary CoA analogue complexes with TpCS have over a 2-fold greater extent. The differences in shapes of spectra may be attributed to contributions from the respective protein chromophores or to slight differences in the conformation of bound ligands.

Fluorescence Spectra of Binary and Ternary Complexes. For PCS, the changes in the fluorescence spectra (excitation at either 280 or 295 nm) induced in the protein emission spectrum by formation of complexes are small and uninteresting (data not shown). On the contrary, with TpCS, large changes in amplitude and shape accompany OAA binding (Figure 3A). A further, but much smaller, change results from formation of the ternary complex with CMCoA. Surprisingly, changes induced by product complex formation are again small; no significant protein fluorescence changes occur on binding CoA, citrate, or both (Figure 3B).

Inhibitor and Substrate Dissociation Constants. Table 1 compares binary and ternary complex dissociation constants for substrates and inhibitors. DethiaAcCoA is a sulfurless ketone analogue of the substrate AcCoA and is competent to undergo efficient enzyme-catalyzed proton transfer from its methyl group (*24*). Although exchange requires OAA, dethiaAcCoA does not react further by condensing with OAA to form a ketone analogue of CitCoA (*24*). CMCoA is a tight-binding analogue of the enolate intermediate/transition state of AcCoA (*26*, *27*, *37*). TpCS binds most substrates and products more tightly than PCS but the affinity of its OAA binary complex for the intermediate analogue is about the same.

NMR Probes of OAA and AcCoA Activation. Table 2 gives the chemical shift data for [2-^{13}C]-OAA and [1-^{13}C]-CMCoA (AcCoA enolate analogue) bound in PCS and TpCS binary and ternary complexes, as well as the chemical exchange regime (free ligand exchanging with ligand in the complex). There is substantial deshielding (~7 ppm) of the carbonyl carbon of OAA when bound in the ternary complex of either CS with CMCoA, the enolate analogue inhibitor. CMCoA's carboxyl carbon is shielded by ~2 ppm and CMCoA is in slow exchange with excess ligand in these ternary complexes.

Table 2: Chemical Shifts and Exchange Regime (Ternary Complexes) of [2-^{13}C]OAA and [1-^{13}C]CMCoA for Complexes of PCS and TpCS[d]

enzyme	CS−OAA* [b] (ppm)	CS−OAA*−CMCoA (ppm)	CS−CMCoA* (ppm)	CS−OAA−CMCoA* (ppm)
none		199.8[c]	178.1(-COO$^-$), 174.9(-COOH)[d]	
PCS	204.4[c]	206.6[c] (slow exchange)	177.4[d] (fast exchange)	175.2[d] (slow exchange)
TpCS	202.1	205.8 (slow exchange)	nd	174.9 (slow exchange)

[a] Apparent pH values (pH*) were 7.5, relative to H_2O standard buffers. No correction was applied for the 25%/V D_2O content. [b] The asterisk indicates the labeled ligand. [c] Reference *43*. [d] Reference *26*.

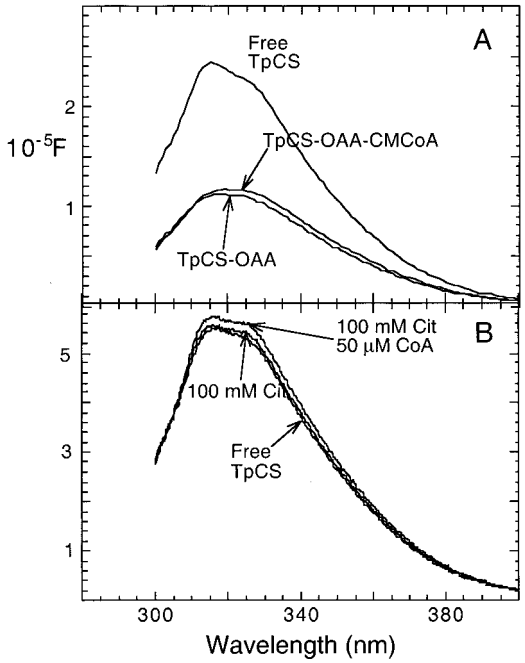

FIGURE 3: Fluorescence spectra of TpCS and some of its complexes. (A) From the top: TpCS (no ligand 1.36 μM, excitation at 290 nm), TpCS−OAA−CMCoA (1.36 μM TpCS, and 100 μM OAA, and 4 μM CMCoA), TpCS−OAA (1.36 μM TpCS and 100 μM OAA). (B) From the top: TpCS−Cit−CoA (1.36 μM TpCS, 100 mM citrate, and 50 μM CoA), TpCS−citrate (1.36 μM TpCS and 100 mM citrate), TpCS (no ligand, 1.36 μM).

k_{cat}s for AcCoA/OAA, CoA/Citrate, and CitCoA. Table 3 compares the k_{cat} values of the enzymes with the various substrates and the CitCoA partitioning ratio at pH 8.0 and 20 °C. The partitioning ratio of CitCoA as substrate is calculated as the initial rate for production of reactants (OAA detected by the MDH reaction) divided by the initial rate for production of products (CoA detected by the DTNB reaction). Solvent and substrate deuterium isotope effects are also tabulated as determined under conditions noted in the table.

pH and Temperature Dependencies of k_{cat}s for AcCoA/OAA, CoA/Citrate, and CitCoA and the CitCoA Partitioning Ratio. Figure 4 shows the k_{cat} values for AcCoA and CitCoA as substrates for TpCS over a pH range of 5.5−10. The pH ranges covered by the various buffers overlap by at least one value. For phosphate buffers and low-pH buffers, progress curves for AcCoA/CitCoA were zero-order over a smaller percentage of the time course than with other buffers. Runs at two AcCoA concentrations (100 and 200 μM) were used to ensure that the rate constants reported reflect true rates at saturation. The lack of pH dependence simplifies the interpretation of solvent isotope and temperature effect (vide infra).

The reverse reaction for TpCS was studied between pH 6 and 8 (inset in Figure 4) and the k_{cat} was found not to depend on pH over this range. In D_2O solutions, between pD 6.4 and 8.4 the k_{cat} also remained constant, albeit at a value 1.8-fold lower (data not shown). Thus, the interpretation of the solvent isotope effects on the reverse reaction is not complicated by ionizations of the ES complexes.

Table 3: Turnover Numbers (min^{-1}), Substrate and Solvent Isotope Effects[a]

	PCS[b]	TpCS
k_{cat}(AcCoA) (min^{-1})	10 000 (pH 7.5)	550 (pH 8)
k_{-cat}(Cit,CoA) (min^{-1})	282[c] (pH 6)	0.73 (pH 8)
k_{cat}(CitCoA) (min^{-1})	≥7000[d]	550 (pH 8)
V_i^{OAA}/V_i^{CoA} [e]	0.4[f]	0.03
$^{D}V_{AcCoA}$	1.40 ± 0.03[g] (H_2O)	1.17 ± 0.03 (H_2O)
	1.12 ± 0.03[g] (D_2O)	1.17 ± 0.04 (D_2O)
$^{D_2O}V_{H3AcCoA}$	2.40 ± 0.08[g]	2.41 ± 0.07
$^{D_2O}V_{D3AcCoA}$	2.70 ± 0.08[g]	2.33 ± 0.07
$^{D_2O}V_{Cit,CoA}$ (reverse)	2.05[h]	1.80 ± 0.20
$^{D_2O}V_{CitCoA}$	nd[i]	2.80 ± 0.15

[a] Data reported were obtained at 20 °C except for the PCS isotope effect data, which were obtained at 22 °C. See ref *72* for detailed discussion of the symbolic representation for the various isotope effects. [b] In general, the values for the isotope effects for PCS can only be approximately correct. At the time these studies were done (*36*), it was not fully appreciated that exchange of the methyl protons of AcCoA with those of solvent can occur within the ternary complexes (*5*, *38*). This is the same reason that the value of the intrinsic isotope effect of 2.0 determined by intramolecular competition using chiral methyl AcCoA must be regarded as a lower limit on the actual value. [c] Calculated from data in ref *34* which were obtained at 22 °C. [d] Estimated from initial burst rate (*6*). Kinetic cooperativity with PCS makes a quantitative estimate difficult (*28*). [e] V_i^{OAA}/V_i^{CoA} = CitCoA partitioning ratio. For TpCs, $k_{OAA} = 24$ min^{-1} and $k_{CoA,Cit} = 660$ min^{-1}. [f] References *6* and *5*. [g] Calculated from Table 2 of ref *36*. Note that solvent exchange with the hydrogens of the methyl group of AcCoA makes difficult the interpretation of solvent isotope effects with PCS. [h] Calculated from Figure 3 of ref *36* at their respective pH(D) optima. [i] Kinetic cooperativity makes a determination difficult to interpret.

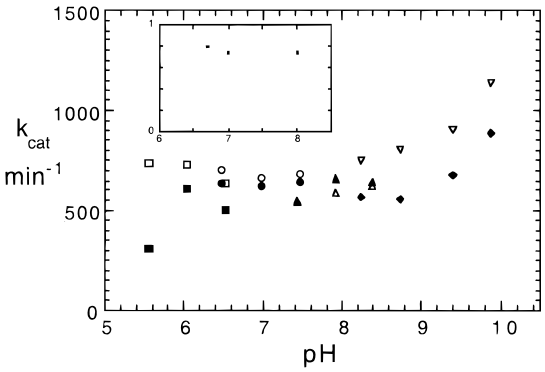

FIGURE 4: pH dependencies of TpCS k_{cat}s for AcCoA/OAA, CitCoA, and CoA/citrate at 20 °C. Solid symbols are for AcCoA/OAA; open symbols are for CitCoA. Squares are 50 mM MES buffer, circles are 50 mM phosphate buffer, triangles are 50 mM EPPS buffer, and inverted triangles are CHES buffer. The pHs of reactions were measured in the cuvettes after completion of the reaction. Inset: k_{cat} for the reverse reaction with CoA and citrate as substrates.

Table 4: Solvent Exchange Rates and Extents for Citrate Synthase

	exchange rate into CH_3 moiety[a]		deuterium excess in citrate		
				CitCoA-d_0	
enzyme	dethia-AcCoA	AcCoA	AcCoA and OAA-d_2	OAA release reversible	OAA release irreversible
PCS[b]	0.48	ND[c]	0.36	0.23[d]	0.14
PCS H320Q[b]	0.03	≤0.05	0.18	ND	ND
PCS H320G[b]	0.06	1.0	0.59	ND	ND
PCS H320N[b]	0.11	1.2	1.4	ND	ND
PCS D375E[b]	2.7	0.6	1.25	1.5[d]	0.65
TpCS[e]	1.0	ND	ND	ND	ND

[a] Relative to reaction rate with AcCoA under the same conditions. [b] References *38* and *5*. [c] None detected. [d] Significant peaks for citrate-d_3 and -d_4 are present in citrate produced from d_0CitCoA with D375E but none with WT PCS. [e] This work.

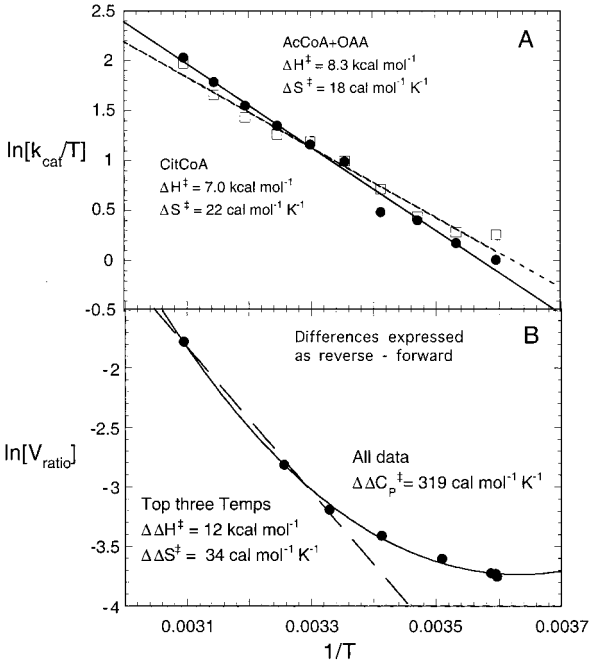

FIGURE 5: Temperature dependencies of TpCS k_{cat}s for AcCoA and CitCoA and partition ratio. (A) Solid line is the linear least-squares fit for data with AcCoA/OAA as substrate. Dashed line is the linear least-squares fit of data with CitCoA as substrate. Thermodynamic constants are calculated from the slope and intercepts of the linear least-squares fits. (B) Dashed line is the linear least-squares fit of partition ratio data for three highest temperatures. Solid line is the nonlinear regression fit of all partition ratio data to eq 1.

The temperature dependencies of k_{cat}s for AcCoA/OAA and CitCoA for TpCS are shown as the Eyring plots [ln (k_{cat}/T) vs 1/T] in Figure 5A. No curvature or changes in slope were found. $\Delta H^{\ddagger}$ and $\Delta S^{\ddagger}$ were calculated from the slopes and intercepts. Values of $\Delta H^{\ddagger}$ of 8.3 ± 0.3 and 7.0 ± 0.3 kcal mol^{-1} and values of $\Delta S^{\ddagger}$ of 18 ± 1 and 22 ± 1 cal mol^{-1} K^{-1} are found for AcCoA/OAA and CitCoA as substrates for TpCS, respectively. The instability of CitCoA and OAA renders data collected at high temperatures increasingly unreliable, and the errors quoted from the linear regression may be underestimates.

A plot of natural logarithm of the partition ratio vs 1/T is found in Figure 5B. This plot is quite curved and, as implied by the results above, the curvature in this plot results from the increasing rate of cleavage of CitCoA relative to its hydrolysis (Figure 5A) as the temperature increased. As indicated in Figure 5A, the $\Delta H^{\ddagger}$ for the hydrolysis of the intermediate CitCoA shows no temperature dependence. The partition ratio data were fit by nonlinear regression to

$$\ln k = A\left(\frac{1}{T}\right) + B \ln T + C \qquad (1)$$

A $\Delta\Delta C_p^{\ddagger}$ of 319 ± 19 cal mol^{-1} K^{-1} was obtained from the fitted curve (solid line in Figure 5B). Analyzing the higher temperature data with a linear regression (dotted line in Figure 5B) yielded values of 12 ± 1 kcal mol^{-1} for $\Delta\Delta H^{\ddagger}$ and 34 ± 5 cal mol^{-1} K^{-1} for $\Delta\Delta S^{\ddagger}$.

Rate of Exchange of Solvent Protons into the Methyl Group of AcCoA or DethiaAcCoA. Consistent with the ability to catalyze proton transfer from the methyl group of AcCoA to generate a high-energy enolate intermediate, these enzymes can catalyze exchange of the protons of the methyl group of AcCoA and AcCoA analogues with those of solvent. Data for PCS, some mutants of PCS, and TpCS are given in Table 4. The rates of these exchanges are probes of the rates of proton transfer relative to other processes within the active site, which may include conformational changes modulating the accessibility of the active site to solvent (*5*, *28*, *38*).

CS-Catalyzed Exchange of Solvent Protons into Product Citrate. Even when solvent exchange of the AcCoA methyl protons cannot be detected in substrate AcCoA for whatever reason, exchanged hydrogens from the AcCoA moiety may appear in the methylene of citrate. Using mass spectrometry to assess exchange into the methylene of citrate is sensitive and accurate and allows study of exchange when the initial substrate is the chemical intermediate CitCoA (*5*). The deuterium *excesses* for the exchange reactions for some PCS mutants and wild-type PCS and TpCS are recorded in Table 4; a maximum value of 2.0 (expressed as additional deuterium excess in this case) is possible for reactions starting with OAA-d_2/AcCoA. Reactions starting with OAA-d_2 and CH_3-AcCoA should produce 100% citrate-d_2 if no enzyme-catalyzed exchange occurred while complete exchange would have 100% d_4. (If OAA preexchange is complete, no isotopic species containing less than d_2 should be present.) Starting with CitCoA-d_0 as substrate, it is possible to obtain citrate containing from 0 to 4 deuteriums. OAA released into solution can undergo nonenzymatic exchange to OAA-d_1 or -d_2 and then subsequently react with activated AcCoA containing from 0 to 2 deuteriums.

Results of exchange experiments with CitCoA allow an interesting distinction when they are considered together with the CitCoA partitioning data. If significant amounts of exchange are occurring because the condensation reaction is reversing all the way back to free OAA, then the released OAA will exchange its methylene protons nonenzymatically.

Significant amounts of citrate-d_3 and -d_4 will be obtained when this released OAA reacts with deuterated AcCoA. If all the exchange is occurring without release of substrates bound to the enzymes, then only citrate-d_1 and -d_2 will be obtained. This distinction between exchange occurring from reversal of the entire condensation step back to free reactants vs exchange occurring as a consequence of exchange of bound states was not possible in previous experiments (*38*).

DISCUSSION

PCS and TpCS have nearly identical binding and catalytic residues and very similar secondary, tertiary, and quaternary structures. Data reported here demonstrate that the two enzymes have the same formal kinetic mechanism and use basically the same catalytic strategies at the molecular level. The additional question we have sought to answer in this work is what subtle differences are responsible for the markedly lower catalytic efficiency of TpCS. In the following section we will develop the theme that the differences between the enzymes strongly implicate the increased rigidity of the thermostable enzyme with a concomitant difficulty in undergoing conformational changes as the underlying cause of catalytic inefficiency in TpCS. Evidence has previously been presented suggesting an inverse relationship between the impact of changes in conformational flexibility on protein stability and enzymatic catalytic efficiency (*39*).

Catalytic Strategies Are the Same for PCS and TpCS. These include carbonyl polarization, the generation of a nucleophilic intermediate/transition state from the methyl group of AcCoA, and the sequence of macromolecular conformational changes between several open and closed forms that are integral steps of the catalytic cycle.

Carbonyl polarization is a general strategy used by many enzymes that catalyze reactions involving nucleophile attack on an electrophilic carbonyl carbon. By increasing the positive charge at the reaction center, these enzymes increase reactivity for condensation with the nucleophile derived from AcCoA in the case of citrate synthases. Several in the long list of enzymes utilizing carbonyl polarization [TIM (*40*), LDH (*41, 42*), and PCS (*31, 43*)] have a similar constellation of positively charged residues surrounding the carbonyl. Since this constellation is also present in TpCS, it may be responsible for a local electrostatic potential increasing the carbonyl carbon's electrophilicity toward the AcCoA nucleophile.

Experimental techniques demonstrating carbonyl polarization of OAA bound to citrate synthase detect the decreased electron density around the carbonyl carbon [increased chemical shift in carbon NMR spectra (*5, 28, 43*)] or the consequent reduced double-bond character [decreased carbonyl stretching frequency in IR spectra (*31*)]. While already apparent in binary CS−OAA complexes, the maximal carbonyl deshielding is seen in ^{13}C NMR spectra of ternary complexes of [2-^{13}C]-OAA with AcCoA analogues, particularly the enolate analogue, CMCoA. As seen by the closely similar chemical shifts for the OAA carbonyl carbon in CMCoA complexes (Table 2), TpCS is able to polarize the OAA carbonyl as well as PCS.

The nucleophile in the CS reaction is derived from the methyl group of AcCoA. Both CS enzymes catalyze proton transfer from the methyl group to generate either an *enolate/carbanion intermediate or transition state.*

Evidence for the existence of this intermediate/transition state carbanion includes tight binding of structural, albeit stable, analogues of this high-energy species. In comparison with ground-state analogues, stable analogues of an intermediate or transition state that possess its critical features will exhibit some of the enzyme's extraordinary affinity for these high-energy states (*44*−*46*). The critical structural features of the enolate/carbanion are the planar sp^2 geometry of the nucleophile carbon and its negative charge. CMCoA (and the related compound CMX) mimic these features (*27, 47*). The tight binding of CMCoA (Table 1) to both PCS−OAA and TpCS−OAA complexes is strong evidence that the same enolate/carbanion of AcCoA is the high-energy intermediate/transition state for both enzymes.

Other evidence for the carbanion/enolate intermediate/transition state is the abilities of the two enzymes to catalyze exchange of the methyl protons of substrate or substrate analogues at a rate comparable to turnover. Table 4 shows exchange data.

The exchange results with the substrate analogue (dethiaAcCoA) are particularly easy to interpret. DethiaAcCoA does not react further to condense with OAA to form a ketone analogue of CitCoA (*24*) and thus it is possible to study the proton-transfer step in isolation. While both enzymes are efficient catalysts of proton transfer from a carbon acid as monitored by dethiaAcCoA exchange, relative to their overall k_{cat}s, exchange is more rapid with TpCS than with PCS (Table 4). The increased exchange rate relative to turnover for TpCS is consistent with the conclusion (vide infra) that the proton-transfer step in TpCS is less rate-limiting to the overall turnover rate than it is in PCS.

Exchange during actual turnover is sensitive to the relative rates of several processes within the ternary complex. Failure to detect exchange in the free AcCoA substrate pool while detecting it in the citrate methylene (Table 4) can result from a substantial commitment to catalysis after the proton-transfer step. The exchanged AcCoA bound to the enzyme reacts further before it has a chance to dissociate from the enzyme. This describes the situation with WT PCS (*5, 38*). In contrast, TpCS fails to catalyze solvent proton exchange into *either* the AcCoA methyl or citrate methylene. Combined with the failure of TpCS to cleave CitCoA to OAA/AcCoA at a significant rate, the failure of TpCS to catalyze exchange during turnover is a consequence of functional irreversibility of *both* the condensation producing the chemical intermediate and the proton-transfer step itself (vide infra).

Unusual Hydrogen-Bonding Structures Involving the Enolate Analogue and Catalytic Residues Are Present in Both Enzymes. For PCS, solid-state NMR (*9*) and structural studies (*47*) have found the hydrogen bond between the carboxyl oxygen of the active site base (D375) and the carboxyl oxygen of the enolate−analogue inhibitor to be extremely short (O−O distance < 2.4 Å) and to possess unusual geometry. The solid-state NMR studies have unequivocally demonstrated that the carboxyl of the analogue is an anion. The hydrogen bond between the oxygen of the inhibitor and the active-site base is in the less basic anti conformation relative to the inhibitor's carbonyl, while it is in the more basic syn conformation relative to the carbonyl of the active-site base, D375 (*9, 47, 48*). This geometry is consistent with the role of the active-site base in the actual enolate intermediate−active-site base complex. This hydrogen-bond

arrangement is responsible for the shielded isotropic chemical shifts of the carboxylate of the enolate analogue observed in NMR spectra of CS−OAA−CMCoA complexes (Table 2). In comparison to a carboxylate anion in solution, the NMR isotropic chemical shifts of the CMCoA/carboxylate carbon bound in these complexes is shielded almost as much as the protonated (COOH) species in solution. Nearly identical isotropic chemical shifts are observed for this carbon in ternary complexes with both enzymes.

It is worth noting that despite the short heteroatom−heteroatom distance (*47*) and the evidence for proton uptake upon complex formation (*26, 37*), this is not a low-barrier hydrogen bond stabilizing an *enol* inhibitor analogue as originally proposed (*12, 49*). The negative charge resides on the carboxylate of the inhibitor and the proton is bound to the oxygen of the active-site base (*9*). This conclusion does not rule out the possibility that the actual (unstable) intermediate is an enol since stable CMX and CMCoA analogues cannot fully mimic the actual unstable species.

Conformational changes and the required underlying protein flexibility are integral parts of the catalytic strategy of CS. Many of the activated substrates and chemical intermediates implicated in the mechanism of citrate synthase either could not form or would be too unstable in the presence of bulk solvent water. Successive conformational changes must thus occur to admit or exclude substrates and water from the active site during the catalytic cycle. The enzymes catalyze two kinds of reactions of thioesters (ligase and hydrolase) within the same active site with the same catalytic residues, certainly requiring further subtle conformational rearrangements.[3,4] Solution and structural evidence supports the existence of comparable conformational states for both PCS and TpCS.

X-ray structure results have captured a static picture of some of these conformers. The X-ray structures of CS fall into either of two conformational classes (*21, 50*). The "open" forms of the enzyme have free access of solvent to the active site and are believed to function in substrate/product binding and dissociation. The various "closed" forms totally exclude bulk solvent with the active site over 15 Å from the nearest surface water contact. All of the chemical transformations are believed to take place in closed forms. The conversions of the "open" to "closed" forms results from a *net*[4] rotation of the small domain of one subunit with respect to the large domain of the other. Structural evidence supports the same kinds of conformation forms in TpCS. The TpCS structure presently available is in the open form (*20*) but two other archael citrate synthase structures are in a closed form with bound products (Figure 1), citrate/CoA (*13, 14*). In addition, at the primary sequence level, several residues implicated in the conformation change in PCS are also present in TpCS. Several PCS residues have been identified as "hinge" residues with respect to the relative motion of the two domains (*1, 3, 15, 47, 50*−*52*). In PCS, changes at these sites destroy the capacity to carry out the overall reaction (*53*). All of the hinge residues are conserved in TpCS (*20*).

Solution studies (UV, CS, fluorescence, and NMR) also give some insight into the nature and dynamics of conformational changes in the two enzymes. The conformation change that is initiated by OAA binding has been detected by changes in UV difference spectra (*35*) and in high-wavelength CD spectra of the enzymes (*5, 26*). When OAA binds to the enzymes, the CD signal intensity generally increases over the entire near-UV region (Figure 2). This presumably reflects a reduction of freedom of motion relative to the chiral peptide backbone of the side-chain aromatic chromophores of tryptophan, tyrosine, and phenylalanine, which absorb in this region. PCS mutants (H320R,N,G,Q (*5, 28*)] for which the formation of the hydrogen bond between the residue at 320 and the OAA carbonyl is made difficult or impossible show no change in their CD spectra with OAA binding. NMR studies of these same PCS mutants show the polarization of the carbonyl also requires this hydrogen bond. Preliminary studies of a TpCS mutant in the active-site histidine analogous to PCS H320 support the importance of this residue for TpCS as well (Kurz et al., 1999, unpublished data).

The fluorescence changes accompanying the binding of OAA to TpCS (Figure 3) strengthen our hypothesis that the OAA binary complex is a closed or partially closed conformer. The emission spectrum of TpCS has its main emission peak at 315 nm and a pronounced shoulder around 328 nm, reflecting the presence of several tryptophan residues with varied exposure to solvent. In comparison to the free enzyme spectrum, that of the OAA complex has a greatly reduced overall intensity and is missing the long-wavelength shoulder. Of the four W residues found in the unliganded enzyme, one is exposed (W17) and two seem to be mostly buried (W115 and W245). W348 lines the active site pocket and in the absence of substrates is likely accessible. In the closed form, however, W348 will become inaccessible (*20*) and its emission should shift to the blue, as is observed (Figure 3).

Conformational changes are also detected when the other possible binary complexes (CS−citrate, CS−CoA analogue) are formed. Thus, CD changes accompany the binding of citrate to both PCS and TpCS (Figure 2). However, quantitatively, the changes are not the same as those induced by OAA binding, and most telling is the absence of any change in the fluorescence spectrum of TpCS induced by formation of the citrate binary complex (Figure 3). This observation suggests that the citrate complex is open. Indeed, the citrate complex of PCS crystallizes in the open conformation (*21*). The induced CD in the binary citrate complex may reflect increased rigidity of an open form or a dynamic equilibrium between open and closed forms that is easily perturbed by crystal forces.

The binary complexes of PCS with CoA analogues have only about half the CD intensity change at 260 nm as the ternary complexes (Figure 2). Less immobilization of the chromophore against the chiral surface might reflect either an open form structure for these complexes or a complex with increased flexibility. Rapid exchange of the ligands on the NMR time scale is consistent with an open form structure (Table 2). In comparison, the extents in TpCS binary CoA complex CD spectra are significantly greater, close in magnitude to PCS ternary complexes. Binary TpCS com-

[3] The only evidence ever found for futile hydrolysis of AcCoA occurs in the D375G PCS mutant, which has negligible activity.

[4] The CS open−closed conformation change involves more than just a rigid-body rotation of the two domains. There are substantial changes in the packing of interior side chains (*1, 2*). At least three types of closed structures have been identified in solid-state structures (*1, 3*) and in solution spectroscopic studies (*4, 5*).

Scheme 1

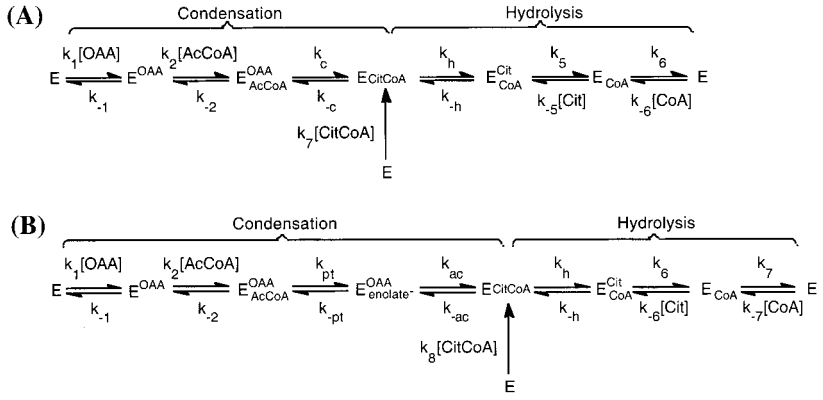

plexes seem generally more "closed" than PCS complexes. Structural data show that even the "open" form structure determined for unliganded TpCS is more "closed" than the corresponding structure for PCS (*20*). For PCS, a net rotation of the small domain relative to the large by 19° is required to interconvert the open and closed forms. TpCS requires only a 12° rotation.

Ternary complexes and binary complexes containing binding determinants from both substrates are in the "closed" form. Their formation is accompanied by the largest induced CD signal in the adenine absorption of the bound CoA analogue. CD spectra of substrate analogue ternary complexes, intermediate analogue ternary complexes, and product ternary complexes are all very similar but not identical and are detecting subtle differences in conformation. The NMR studies of these complexes (Table 2) also show the bound ligands to be in slow exchange (on the NMR time scale). All the crystal structures of citrate synthase ternary complexes are closed forms (*13*, *14*, *20*, *50*, *54*).

While the above results argue that corresponding conformational changes occur for both enzymes, it must be kept in mind that conformation change during the catalytic cycle is a dynamic process. While the solid-state structures have given valuable insight, they have limited usefulness in determining either the rate of interconversion or the position of equilibrium between conformers. Supporting the existence of a dynamic equilibrium between conformers is the observation (*3*) that both open and closed PCS forms can crystallize from a single drop containing CoA and citrate (1 M). Various conformational forms also differ in the flexibility of side chains [arguing from differences in temperature factors (*3*), which seem to depend on the identity of bound ligands]. A dynamic equilibrium between more than one form of OAA binary complex has been invoked to explain OAA carbon line widths in NMR spectra of the binary complex (*43*).

Structural data indicate less overall flexibility in the citrate synthases isolated from thermophiles (*14*, *20*). Solution data also indicate increased rigidity. We were impressed by the large increase in the amplitude of the induced CD signals in the CoA analogue binary and ternary complexes of TpCS when compared to the amplitude of the corresponding complexes in PCS (Figure 2). At the same temperature of 20 °C, the dissociation constants of TpCS complexes (Table 1) almost uniformly reflect tighter binding. To the extent that stronger interactions between enzyme and ligand groups indicate a more strongly immobilized final state, then this trend in the binding data is certainly consistent with our picture of the complexes of the thermophile enzyme as rigid, less flexible species.

The Formal Kinetic Mechanisms of the Two Enzymes Are Very Similar. The relative values of substrate binding constants (Table 1) support a preferred ordered bi-bi mechanism in the forward direction with OAA binding first. In addition, for both PCS (*50*) and TpCS (*20*), the structural data show that if CoA bound first, it would sterically interfere with subsequent OAA binding.

CitCoA Is a Stable Intermediate in the Catalytic Cycle of Both Enzymes. Supporting data are the rapid initial rates of CitCoA hydrolysis by both enzymes. The very high affinity of the two enzymes for the intermediate suggests that it is never released into solution during normal turnover.

CitCoA as a substrate for PCS shows kinetic cooperativity yielding a complex pattern of kinetic phases with widely differing rates (*5*, *6*, *28*), with the initial rate of the burst phase approximately equal to the turnover rate. The lack of substrate concentration dependence of the burst rate indicates tight binding. All the models explaining the kinetic cooperativity observed with PCS require tight binding of CitCoA (*6*, *28*).

There is no kinetic cooperativity in TpCS-catalyzed CitCoA hydrolysis. The very tight binding of CitCoA to the TpCS enzyme is indicated by the zero-order nature of progress curves and the virtual independence of the values of the initial rates on CitCoA concentration.

The mechanistic significance of kinetic cooperativity in PCS and it absence in TpCS is unknown. However, its absence is perhaps another symptom of increased rigidity of TpCS since kinetic cooperativity (allostery) is presently understood by models requiring dynamic equilibria between conformational forms (*55*, *56*).

The relative stabilities of internal states differ substantially for the two enzymes, even to the extent that the rate-determining step is changed and the condensation step, which is reversible for PCS, becomes almost irreversible for TpCS. This occurs despite the identities of catalytic groups and the similarity of their overall mechanisms.

We will discuss the kinetic mechanism using Scheme 1. This scheme shows kinetic mechanisms for an ordered bi-bi reaction with a ternary interconversion occurring with two (A) or three (B) steps. The schemes omit separate steps related to conformational changes as well as several possibly reversible steps during hydrolysis (*38*). In Scheme 1A, the

overall condensation step producing CitCoA is given rate constants k_c and k_{-c}, while the hydrolysis step is given the rate constants k_h and k_{-h}. In Scheme 1B, the overall condensation step is represented as two steps in which the proton transfer (k_{pt} and k_{-pt}) from AcCoA to generate an enolate intermediate occurs first, followed by the actual condensation (k_{ac} and k_{-ac}) with the OAA to give the relatively stable intermediate, CitCoA.

It is clear that no single step is rate-determining for PCS. Despite the limitations imposed on analysis by kinetic complexities,[5] Pettersson et al. (*6*) have developed a kinetic model for PCS that is consistent with the values of the kinetic constants and CitCoA partition data. In this model, condensation is readily reversible with an internal K_{eq} value of about 1; hydrolysis is the slowest step but only by about a factor of 10. Other data support this picture. The observed substrate isotope effect (deuterium substitution in the methyl group of AcCoA) is quite small [Table 3 (*36*)], substantially lower than would be expected if proton transfer was mainly rate-limiting. The lower limit (*5*) on the value of the intrinsic primary isotope effect on proton transfer in the PCS reaction was determined to be about 2 from intramolecular isotope effect measurements using chiral methyl-AcCoA (*57, 58*). The further diminishment of the value of the observed substrate isotope effect when it is measured in solvent D_2O (Table 3) suggests that barriers for the steps affected by substrate and solvent isotopes are not greatly different in height. Given that proton transfer from carbon is thermodynamically and kinetically difficult in small molecule models (*49, 59*), we were surprised that this step presents such a small barrier in both the CS-catalyzed reactions.

The Internal Steps, Which Generate Intermediates, Are Readily Reversible in the PCS Reaction. CitCoA is the most stable of these intermediates. The initial[6] *ratio* of the rate of CitCoA cleavage to hydrolysis for PCS is 0.4 (*5, 6, 60*), indicating that while hydrolysis is somewhat favored over cleavage, the condensation step is readily reversible. Most if not all of the exchange with solvent protons appearing in the methylene of citrate product (under conditions of irreversibility of the overall reaction) comes from reversal of the condensation all the way back to bound OAA/AcCoA (*5, 38*).

Data supporting existence and reversible formation of a discrete enolate intermediate in PCS WT are considerably weaker. Reversal of the proton-transfer step alone can lead to exchange, as we have already observed in the case of dethiaAcCoA. Our current hypothesis is that proton transfer and condensation are concerted for all practical purposes in wild-type PCS. However, if condensation is made sufficiently difficult, as in mutants with impaired OAA polarization (or for the case of the dethiaAcCoA substrate analogue), a decoupling of these steps certainly occurs and extensive exchange may sometimes be observed [Table 4 (*5, 24*)].[7]

Unlike PCS, TpCS Has a Clear Rate-Determining Step, the Hydrolysis of CitCoA. The k_{cat} starting with AcCoA/OAA as substrate is very close in value (within about 5%) to the k_{cat} with CitCoA (Table 3, Figures 4 and 5A). This identity is not an accident of experimental conditions because pH (Figure 4) and temperature dependencies (Figure 5A) of both k_{cat}s are nearly identical. For initial velocities in the forward direction, the dissociation constants for both TpCS (and PCS) suggest that product off rates are not kinetically significant (Table 1). Under these circumstances the k_{cat} is given by

$$k_{cat} = \frac{k_c k_h}{k_c + k_{-c} + k_h} \approx k_h \quad \text{if} \quad k_h, k_{-c} \ll k_c \tag{2}$$

k_{cat} (AcCoA/OAA) can equal k_{cat} (CitCoA) $= k_h$, only if k_{-c} and k_h are much less than k_c.

The lack of significant pH dependence of the k_{cat}s for TpCS is a consequence of the nature of its rate-determining hydrolysis step. The only active-site residue implicated in the hydrolysis is D375, whose carboxylate side chain is apparently acting as a general base. This carboxylate should remain ionized over the experimental pH range. The pH independence of the k_{cat}s follows. The high p*I* (vide supra) of TpCS strongly suggests that one or more histidine active-site residues either do not ionize in the expected pH range or, if compensating charge changes occur, they do not affect the rate constant for hydrolysis.

PCS shows a much more normal pH dependence, having bell-shaped pH−rate profiles with maxima at pH 8 for k_{cat} of the forward reaction and near pH 6 for k_{-cat} of the reverse reaction. The pH dependence of PCS is not easily interpreted in terms of specific residues but is consistent with rate contributions from additional steps (condensation). The condensation involves several residues [certainly including H320, H274, and H238 as well as D375 (*5, 61*)] that are either likely or required to change protonation states during the catalytic cycle.[8]

[5] PCS shows a number of complexities that allow only a limited disentanglement of the kinetic constants into rate constants for individual steps in the mechanism (*5, 6*). Most notable complexities are the exchange of solvent protons into the methyl of substrate and methylene of product and the kinetic cooperativity with CitCoA as substrate. The first complicates the interpretation of substrate and solvent isotope effects because isotope can be lost or gained in the substrate. The second complicates the measurement of the partition of the chemical intermediate between the forward and reverse reactions.

[6] The initial rate referred to here is in the burst phase.

[7] The proposed enolate intermediate resulting from proton transfer from AcCoA must be very unstable and its lifetime before the actual condensation must be short. In some circumstances the lifetime of intermediates may be so short that their existence as a separate species can be debated (see ref *7*) for an informative discussion of "when an intermediate is an intermediate"). Successful simulations of the exchange experiments (*5*) require the rate constant for a separate condensation step (k_{ac} in Scheme 1B) to be ≥100 fold greater than the rate constant for the reverse proton transfer (k_{-pt}).

[8] The active sites of both citrate synthases contain homologous essential histidine (*3*) and aspartate (*1*) residues. Histidine residues normally titrate in the pH 6−8 range. Steps involving the active-site histidines would be expected to show some pH dependence over the studied pH range, as in fact is observed in the k_{cat} for PCS WT. We also expect the states of ionization of several catalytic residues to change during the catalytic cycle itself. The carboxylate side chain of Asp375 accepts a proton from the methyl of AcCoA in the condensation reaction and is thus at least transiently protonated. It acts again as a general base catalyst in the hydrolysis reaction (*5, 8*). The imidazole side chains of His320, His274, and His238 appear to be neutral, judging from their hydrogen-bonding pattern in a number of crystal structures. Yet the protonated form of H320 is the logical choice to donate a proton to the carbonyl of OAA to form the alcohol of citrate. H274 lies at the amino terminus of an α-helix and should be neutral, although a convincing argument has been made that it is protonated in the D375G mutant (*9*). Theoretical calculations (*10*) indicate that a positive charge on H238 is necessary to stabilize the enolate despite the contrary inference from the structural data.

The *substrate and solvent isotope effects* are also consistent with a single rate-determining step (hydrolysis) for TpCS and several kinetically significant steps for PCS.

In the case of TpCS a more detailed analysis is possible since no isotope is lost through exchange with solvent (Table 4). The substrate isotope effect is given by

$$^{D}k_{cat} = \frac{^{D}k_c + \frac{1}{k_h}(k_c + k_{-c}\,^{D}K_{c,eq})}{1 + \frac{1}{k_h}(k_c + k_{-c})} \approx \frac{^{D}k_c + \frac{k_c}{k_h}}{1 + \frac{k_c}{k_h}} \qquad (3)$$

The elimination of k_{-c} and the terms multiplied by it follows because its value is known to be small from CitCoA partition data (Table 3, vide infra). Even if the equilibrium isotope effect on proton transfer is normal, its value is unlikely to affect this conclusion.[9] Since the remaining term in the numerator and denominator (k_c/k_h) is likely to be substantially greater than 1, a commitment is likely to reduce the observed substrate isotope effect well below the intrinsic value, as is observed. Note that if the proton transfer and actual condensation take place in discrete kinetic steps (Scheme 1B), then an additional commitment may contribute to reducing the observed isotope effect.

If $^{D}k_c$ is ≥ 2 (*5*, *57*), then the observed value of $^{D}k_{cat}$ of 1.17 implies that $k_c/k_h \geq 5$. Almost certainly these are lower limits on both quantities ($^{D}k_c$ and k_c/k_h). Use of D_2O (which raises the barrier for k_h) does not affect the observed value of $^{D}k_{cat}$ (Table 3). When k_h is reduced by a solvent isotope effect of 2 (Table 3), a value of k_c/k_h as low as 5 would make k_{cat}(AcCoA, OAA) less than k_{cat}(CitCoA) by about 17%, a difference that is much larger than we observe ($\leq$5%). So the commitment ratio reducing the substrate isotope effect must be significantly greater than 5.

The *solvent isotope effects* on TpCS k_{cat}s are also consistent with rate-determining hydrolysis. It is reasonable to assume that any significant isotope effect can be attributed to the rate-determining step. We just presented the case that the observed solvent isotope effect for TpCS is associated with a single step, which is *not* the condensation step. For TpCS, the size of the solvent isotope effect is not affected by use of deuterated AcCoA, nor is the size of the apparent substrate isotope effect changed by the use of D_2O as solvent (Table 3). The latter observation confirms a single rate-limiting step for TpCS and contrasts with the behavior of PCS, where more than one step is kinetically significant.

It has generally been assumed that the hydrolysis step involves general acid−base catalysis by the carboxylate side chain of D375 (*5*). A significant solvent isotope effect is likely to be associated with this general acid−base catalysis. Admittedly, there are many other steps in this and other enzyme-catalyzed reactions that might be subject to solvent isotope effects, including conformational changes (*62*). Neglecting this possibility and assuming rapid product dissociation, the solvent isotope effect on k_{cat} is given by eq 4 and has a value of 2.3 in Table 3:

$$^{D_2O}k_{cat} = \frac{^{D_2O}k_h + \frac{k_h}{k_c + k_{-c}}}{1 + \frac{k_h}{k_c + k_{-c}}} \approx \frac{^{D_2O}k_h + \frac{k_h}{k_c}}{1 + \frac{k_h}{k_c}} \qquad (4)$$

The sizes of the commitment terms reducing the observed solvent isotope effect are likely to be modest. We know that k_{-c} is small (vide infra) and this term may immediately be dropped in comparison to the value of k_c. Thus the major commitment reducing the solvent isotope effect, k_h/k_c, is the inverse of that reducing the substrate isotope effect (eq 3). We just showed above that this term $k_c/k_h \geq 5$. So this would imply that the inverse has a value ≤ 0.2.The observed solvent isotope effect is then close in value to the intrinsic effect on the hydrolysis step.

More information may be obtained from specific rates for production of products when CitCoA is used as substrate and will be used to demonstrate the consistency of our kinetic model. The isotope effect for $^{D_2O}k_{cat}^{CitCoA}$ is simply equal to $^{D_2O}k_h$ for the mechanism in Scheme 1 (under the assumption of rapid product dissociation). The additional commitment that appears in the expression (eq 4) for $^{D_2O}k_{cat}$, k_h/k_c, arising from the condensation part of the reaction pathway, does not appear. The solvent isotope effect (Table 3) observed for production of CoA from CitCoA is in fact slightly larger than that on the overall reaction with AcCoA/OAA as substrates. With this small difference, the commitment reducing the solvent isotope effect with AcCoA as substrate is then 0.3, in good agreement with the preceding calculation.

TpCS fails to catalyze exchange of solvent protons into the methyl of the substrate acetyl-CoA or into the methylene of product citrate.[10] The low rate of cleavage of the CitCoA intermediate back to reactant AcCoA/OAA indicates that the overall condensation step is not readily reversible. These data require that the condensation of the enolate intermediate of acetyl-CoA with OAA is either concerted or rapid compared to reverse proton transfer (Table 4).

This requirement is dramatically demonstrated by contrasting TpCS results with those from mutants of PCS where one but not both of the steps is irreversible. Like TpCS, the H320 mutants of PCS show little or no cleavage of CitCoA back to AcCoA/OAA—the overall condensation step is irreversible. Consequently, these mutants show no exchange with CitCoA as substrate whether OAA release is reversible or irreversible (Table 4). Some of these mutants show extensive exchange of solvent protons into both the substrate (AcCoA) and products when the reaction is started from AcCoA (Table 4). The only source of exchange with solvent protons in these mutants is reversal of the proton transfer

[9] The value of $^{D}K_{c,eq}$ is estimated to be slightly inverse with a value of 0.91 if the thioester methyl protons in the reactant and the proton of the active-site Asp carboxyl have normal fractionation factors (*11*). If the transferred proton is in a low-barrier hydrogen bond, it could have a fractionation factor as low as 0.4 (*12*); then the value of $^{D}K_{eq}$ could be normal, with a value as great as 2.0.

[10] One cautionary note is that there is the possibility that the accessibility of the protonated active-site base to solvent protons is limited and that the rate of exchange of this protonated base is a kinetically significant step for the overall exchange of solvent protons into substrate and/or products. Slow exchange of the protonated active-site base is unlikely even with TpCS. The TpCS-catalyzed exchange of the methyl of dethiaAcCoA is rapid (Table 4). Preliminary stopped-flow data monitoring the fluorescence change that results from the open−closed conformation change accompanying OAA binding indicate that the conformation change is fast and is not an event separate from the encounter step.

step occurring prior to the actual condensation, so the enolate intermediate must have a finite lifetime. The WT PCS also shows substantial exchange, which is believed to arise mostly from reversal from CitCoA (*5*, *38*). The total absence of exchange for TpCS suggests that proton transfer and actual condensation are very tightly coupled processes in this enzyme. Other things being equal, the presence of a rate-limiting hydrolysis should have led to greater exchange. This is illustrated by another PCS mutant, D375E. D375E has the hydrolysis nearly rate-determining, as does TpCS (CitCoA k_{cat} equals overall k_{cat}). In contrast to TpCS, however, the formation of CitCoA is easily reversed, and moreover CitCoA partitioning actually favors reactant OAA/AcCoA over product CoA/citrate. For this mutant, CitCoA formation reverses many times before going on to products. This results in very high exchange levels (Table 4) under all conditions.

CitCoA Partition Ratio and Solvent Isotope Effect on k_{-cat}. The solvent isotope effect on the reverse reaction, $^{D_2O}k_{-cat}$, can also be explained by Scheme 1A, further demonstrating the consistency of our kinetic model. Before elaborating this conclusion, it is necessary to develop quantitative expressions for the partition ratio, k_{-cat}, and $^{D_2O}k_{-cat}$, the solvent isotope effect on the reverse reaction.

According to Scheme 1A, the partition ratio for CitCoA as substrate is defined as the ratio of the initial velocity of production of OAA to that for CoA. Under the assumption that product dissociation is fast, then the partition ratio is given by

$$\frac{V_i^{OAA}}{V_i^{CoA}} = \frac{k_{-2}k_{-c}}{k_h(k_{-2}+k_c)} \leq \frac{k_{-c}}{k_h} \tag{5}$$

In the reverse direction, it seems less certain that the dissociation of AcCoA (k_{-2}) is fast compared to condensation ($k_{-2} \gg k_c$ or $\gg k_{pt}k_{ac}$, if Scheme 1B applies), but if it is, the velocity ratio gives the simple expression shown on the right of eq 5 for the relative barrier heights immediately leading to and away from the chemical intermediate, CitCoA.

The k_{-cat}, for the reverse reaction, is given by

$$k_{-cat} = \frac{k_{-h}}{\text{denom}} = 0.75\ \text{min}^{-1} \tag{6}$$

$$\text{denom} = \frac{k_{-h}}{k_{-1}} + \frac{k_{-h}}{k_{-2}} + \frac{k_c(k_h+k_{-h})}{k_{-2}k_{-c}} + \frac{(k_h+k_{-h})}{k_{-c}} + 1$$

Since k_{-h} is much less than k_h, k_{-1}, or k_{-2}, then eq 6 simplifies to

$$k_{-cat} = \frac{k_{-h}}{\dfrac{k_h(k_{-2}+k_c)}{k_{-2}k_{-c}} + 1} \tag{7}$$

We recognize the first term in the denominator as the inverse of the partition ratio, so by substituting in the values obtained at 20 °C, we can calculate that $k_{-h} = 21.4\ \text{min}^{-1}$.

The solvent isotope effect on the reverse reaction at 20 °C has a value of 1.8 and, like the solvent isotope effect on the forward direction, is independent of pH over the range from 6 to 8 (inset, Figure 4). By the same argument used previously, we would then assign this solvent isotope effect to the reverse hydrolysis step reduced by commitments, in which case it is given by

$$^{D_2O}k_{-cat} = \frac{^{D_2O}k_{-h} + \left(\dfrac{k_h(k_{-2}+k_c)}{k_{-2}k_{-c}}\right)^{D_2O}K_{eq,-h}}{1 + \dfrac{k_h(k_{-2}+k_c)}{k_{-2}k_{-c}}} \tag{8}$$

The rate constant term in eq 8 is the inverse of the partition ratio and has a value of 27.5. This represents a substantial commitment term reducing the observed value below that of the intrinsic solvent isotope effect on k_{-h}. The equilibrium constant for the reverse of the hydrolysis is given by

$$K_{eq,-h} = \frac{[E\cdot CitCoA]}{[E\cdot CoAS(H)][E\cdot Cit]} = \frac{k_{-h}}{k_h} \tag{9}$$

and

$$^{D_2O}K_{eq,-h} = \frac{^{D_2O}k_{-h}}{^{D_2O}k_h} \tag{10}$$

Estimating the value of the solvent isotope effect on this equilibrium constant is difficult because the values of the fractionation factors required depend greatly upon protonation state and other details of hydrogen bonding of the enzyme-bound species. However, we recognize that within the context of Scheme 1A, and since we know the solvent isotope effect on the forward hydrolysis rate constant, we can express eq 8 in terms of a single unknown, $^{D_2O}k_{-h}$:

$$^{D_2O}k_{-cat} = \frac{^{D_2O}k_{-h} + \dfrac{V_i^{CoA}}{V_i^{OAA}}\cdot\dfrac{^{D_2O}k_{-h}}{^{D_2O}k_h}}{1 + \dfrac{V_i^{CoA}}{V_i^{OAA}}} \tag{11}$$

Substituting in the values from Table 3 and solving for $^{D_2O}k_{-h}$, we obtain a value of 4.3, a completely reasonable number. In the direction of hydrolysis of CitCoA to its products, citrate and CoA, the transition state is early, as expected for an exoergic process like thioester hydrolysis.

While we have no evidence for it, there is certainly the possibility that the solvent isotope effects observed for both the forward and reverse reactions do not refer to a single, simple chemical step. While the hydrolysis reaction of citrate synthase has received relatively little attention from investigators, several mechanisms with intermediates have been proposed (*33*, *63*) and surprising data showing excess oxygen exchange into product citrate during this step have yet to be explained (*38*).

Comparison of the Internal Thermodynamics of TpCS and PCS. Albery and Knowles (*64*) have defined the optimal internal thermodynamics required for maximum enzyme catalytic efficiency: the free energies of all stable internal states must be closely matched, and the internal equilibrium constants will be closer to 1 than are those for the corresponding free solution reactions. The internal free energy barriers will be low and none will be significantly higher than any other; internal steps are fast and readily reversible,

and no step is significantly slower than any other (no rate-determining step).

PCS approximates this ideal (*5, 6*). It is possible to quantitatively reproduce all the values of kinetic constants for PCS (*6*) with a mechanism in which the production of CitCoA is readily reversible with an internal equilibrium constant close to 1. Values of rate constants for the overall condensation and hydrolysis are within a factor of 10 so that no step is overwhelmingly rate-determining. To explain the low levels of solvent proton exchange (*5*), the proton-transfer step is concerted with condensation, or if proton transfer occurs in a separate step to produce a high-energy enolate intermediate, then the reverse proton transfer and the actual condensation step have comparable rate constants.

TpCS enzyme is inefficient in comparison to PCS. Even at 70 °C, the k_{cat} for TpCS is only about a quarter the value for PCS at 37 °C. TpCS falls short of the ideal catalyst in significant ways. The hydrolysis of the stable intermediate CitCoA is nearly rate-determining and the condensation step that produces it is nearly irreversible. The values of the overall k_{cat} starting with the normal substrates, AcCoA and OAA, are close those of the k_{cat} for hydrolysis of the intermediate, CitCoA, over the temperature range at which the latter is sufficiently stable to allow measurements. TpCS overstabilizes the CitCoA intermediate and fails to adequately stabilize the transition state for hydrolysis, leading to a lower catalytic efficiency. Clues to the reasons for this may be found in the temperature dependence of catalytic constants of TpCS.

The Eyring plots [ln (k/T) vs $1/T$] for the k_{cat}s are linear within experimental error (Figure 5A). The $\Delta H^{\ddagger}$ and $\Delta S^{\ddagger}$ values derived from these plots are unremarkable and typical of many reactions in aqueous solution, which typically show enthalpy−entropy compensation. Curvature resulting from the increased reversibility of condensation with temperature is not detectable in the CitCoA plot (within experimental error) but may be responsible for slight differences in apparent thermodynamic constants for the two k_{cat}s.

The marked curvature in the plot of the temperature dependence of the partition ratio [Figure 5B, ln (V_i^{OAA}/V_i^{CoA}) vs $1/T$] arises entirely from the increasing rate of the cleavage of CitCoA relative to its hydrolysis. The $\Delta\Delta C_p^{\ddagger}$ value derived from this plot (Figure 5B) is thus mostly attributable to the $\Delta C_p^{\ddagger}$ of the cleavage. Its high value, 319 cal mol^{-1} K^{-1}, is not unusual for many processes involving macromolecules (*65, 66*). The molecular interpretation is difficult as in other cases. Trivial explanations involve the possibility that the cleavage consists of more than one step whose kinetic contribution varies with temperature. Recall the possible presence of k_{-2} (AcCoA dissociation rate constant) in the expression for the partition ratio (eq 3). If k_{-2} is less than or equal to k_c, then dissociation could make a contribution that results in an erroneously high value of $\Delta C_p^{\ddagger}$. Similarly, it is also possible that the proton transfer and actual condensation steps are increasingly decoupled at higher temperature and this gives rise to curvature in the plot. A final, more interesting possibility is a conformation change with a significant ΔC_p. While a conformation change involving simple hinge motion (hexokinase) did not result in a significant ΔC_p (*67*), the conformation change in citrate synthase is much more complex and cannot be described as a motion of rigid bodies (*2*).[4] Thermodynamic parameters associated with this type of conformation change are not presently available so it is not possible to exclude contributions from conformational changes. Some of these possibilities are amenable to experiment and are currently under investigation.

While the requirement for increased protein thermostability may itself impose conformational rigidity and lower catalytic efficiency, the effects of a high temperature environment on the stability of substrate OAA may cause an additional metabolic constraint on catalytic efficiency. At high temperatures, where the OAA half-time may be measured in minutes, the OAA−TpCS complex is generally stable. Thus the organism may be able to satisfy the need to maintain adequate concentrations of an essential metabolite, OAA, as well as satisfactory rates of synthase turnover by maintaining higher concentrations of a CS protein with a high OAA affinity but somewhat less overall catalytic efficiency.

CONCLUSIONS

TpCS has the same general catalytic strategy and formal kinetic mechanism as PCS, yet it is a considerably less efficient catalyst. Formally, this is a consequence of fact that the chemical intermediate, CitCoA, lies in a deep thermodynamic pit, at the point in the catalytic cycle that requires the enzyme to switch from ligase to hydrolase. There seems to be no static structural or chemical reason for this pit to be deeper for TpCS than for PCS. The active sites and reactions catalyzed are nearly identical. Our attention is focused on the other striking difference between the two enzymes, the decreased flexibility of the thermophile enzyme. It would be possible to hypothesize that discrete steps involving conformational changes associated with high barriers on either side of CitCoA are responsible. Our kinetic model does not require and in fact argues against separable conformation steps at this point. Instead we propose that the tight binding of the reactants to the enzyme structure has imposed a dynamic constraint on the reaction coordinate motion. Dynamic constraints on reaction rates arising from solvent−substrate interactions have received serious attention in the study of small molecule reactions in high-dielectric (water) solvents (*68*). Now convincing evidence has been presented for such constraints in several enzyme systems involving tunneling (*69*). We believe that this will prove to be a general feature of enzyme catalysis and we will be eager to investigate other citrate synthases originating in even more diverse environments.

REFERENCES

1. Wiegand, G., Remington, S., Deisenhofer, J., and Huber, R. (1984) *J. Mol. Biol. 174*, 205−19.
2. Lesk, A. M., and Chothia, C. (1984) *J. Mol. Biol. 174*, 175−91.
3. Liao, D. I., Karpusas, M., and Remington, S. J. (1991) *Biochemistry 30*, 6031−6.
4. Kollmann-Koch, A., and Eggerer, H. (1989) *Eur. J. Biochem. 185*, 441−7.
5. Kurz, L. C., Nakra, T., Stein, R., Plungkhen, W., Riley, M., Hsu, F., and Drysdale, G. R. (1998) *Biochemistry 37*, 9724−37.
6. Pettersson, G., Lill, U., and Eggerer, H. (1989) *Eur. J. Biochem. 182*, 119−24.
7. Jencks, W. P. (1980) *Acc. Chem. Res. 13*, 161−169.

8. Man, W. J., Li, Y., O'Connor, C. D., and Wilton, D. C. (1991) *Biochem. J. 280*, 521−6.
9. Gu, Z., Drueckhammer, D. G., Kurz, L., Liu, K., Martin, D. P., and McDermott, A. (1999) *Biochemistry 38*, 8022−8031.
10. Mulholland, A. J., and Richards, W. G. (1997) *Proteins: Struct., Funct., Genet. 27*, 9−25.
11. Quinn, D. M., and Sutton, L. D. (1991) *Enzyme Mechanism from Isotope Effects*, CRC Press, Boca Raton, FL.
12. Cleland, W. W., and Kreevoy, M. M. (1994) *Science 264*, 1887−90.
13. Russell, R. J., Gerike, U., Danson, M. J., Hough, D. W., and Taylor, G. L. (1998) *Structure 6*, 351−61.
14. Russell, R. J., Ferguson, J. M., Hough, D. W., Danson, M. J., and Taylor, G. L. (1997) *Biochemistry 36*, 9983−94.
15. Remington, S. J., and Usher, K. (1995) *Protein Eng. 8*, 55.
16. Johansson, C.-J., Mahlen, A., and Pettersson, G. (1973) *Biochim. Biophys. Acta 309*, 466−72.
17. Johansson, C. J., and Pettersson, G. (1974) *Eur. J. Biochem. 46*, 5−11.
18. Johansson, C.-J., and Pettersson, G. (1974) *Eur. J. Biochem. 42*, 383−8.
19. Johansson, C. J., and Pettersson, G. (1977) *Biochim. Biophys. Acta. 484*, 208−15.
20. Russell, R. J., Hough, D. W., Danson, M. J., and Taylor, G. L. (1994) *Structure 2*, 1157−67.
21. Remington, S., Wiegand, G., and Huber, R. (1982) *J. Mol. Biol. 158*, 111−152.
22. Burbaum, J. J., Raines, R. T., Albery, W. J., and Knowles, J. R. (1989) *Biochemistry 28*, 9293−305.
23. Sutherland, K. J., Danson, M. J., Hough, D. W., and Towner, P. (1991) *FEBS Lett. 282*, 132−4.
24. Kurz, L. C., Roble, J. H., Nakra, T., Drysdale, G. R., Buzan, J. M., Schwartz, B., and Drueckhammer, D. G. (1997) *Biochemistry 36*, 3981−90.
25. James, K. D., Russell, R. J. M., Parker, L., Daniel, R. M., Hough, D. W., and Danson, M. J. (1994) *FEMS Microbiol. Lett. 119*, 181−6.
26. Kurz, L. C., Shah, S., Crane, B. R., Donald, L. J., Duckworth, H. W., and Drysdale, G. R. (1992) *Biochemistry 31*, 7899−907.
27. Bayer, E., Bauer, B., and Eggerer, H. (1981) *Eur. J. Biochem. 120*, 155−60.
28. Kurz, L. C., Shah, S., Frieden, C., Nakra, T., Stein, R. E., Drysdale, G. R., Evans, C. T., and Srere, P. A. (1995) *Biochemistry 34*, 13278−88.
29. Martin, D. P., Bibart, R. T., and Drueckhammer, D. G. (1994) *J. Am. Chem. Soc. 116*, 4660.
30. Simon, E. J., and Shemin, D. (1953) *J. Am. Chem. Soc. 75*, 2520.
31. Kurz, L. C., and Drysdale, G. R. (1987) *Biochemistry 26*, 2623−7.
32. Riddles, P. W., Blakeley, R. L., and Zerner, B. (1979) *Anal. Biochem. 94*, 75−81.
33. Srere, P. A. (1969) *Methods Enzymol. 13*, 3−11.
34. Kosicki, G. W., and Srere, P. A. (1961) *J. Biol. Chem. 236*, 2560−2565.
35. Srere, P. A. (1966) *J. Biol. Chem. 241*, 2157−65.
36. Kosicki, G. W., and Srere, P. A. (1961) *J. Biol. Chem. 236*, 2566−70.
37. Kurz, L. C., Drysdale, G. R., Riley, M. C., Evans, C. T., and Srere, P. A. (1992) *Biochemistry 31*, 7908−14.
38. Myers, J. A., and Boyer, P. D. (1984) *Biochemistry 23*, 1264−69.
39. Zavodszky, P., Kardos, J., Svingor, and Petsko, G. A. (1998) *Proc. Natl. Acad. Sci U.S.A. 95*, 7406−11.
40. Belasco, J. G., and Knowles, J. R. (1980) *Biochemistry 19*, 472−7.
41. Deng, H., Zheng, J., Sloan, D., Burgner, J., and Callender, R. (1989) *Biochemistry 28*, 1525−33.
42. Deng, H., Zheng, J., Clarke, A., Holbrook, J. J., Callender, R., and Burgner, J. W. N. (1994) *Biochemistry 33*, 2297−305.
43. Kurz, L. C., Ackerman, J. J., and Drysdale, G. R. (1985) *Biochemistry 24*, 452−7.
44. Wolfenden, R. (1969) *Nature 223*, 704−5.
45. Wolfenden, R. (1974) *Mol. Cell. Biochem. 3*, 207−11.
46. Wolfenden, R. (1976) *Annu. Rev. Biophys. Bioeng. 5*, 271−306.
47. Usher, K. C., Remington, S. J., Martin, D. P., and Drueckhammer, D. G. (1994) *Biochemistry 33*, 7753−9.
48. Gandour, R. D. (1981) *Bioorg. Chem. 10*, 169−176.
49. Gerlt, J. A., and Gassman, P. G. (1993) *Biochemistry 32*, 11943−52.
50. Remington, S. J. (1992) *Curr. Top. Cell Regul. 33*, 209−29.
51. Wiegand, G., and Remington, S. J. (1986) *Annu. Rev. Biophys. Biophys. Chem. 15*, 97−117.
52. Karpusas, M., Branchaud, B., and Remington, S. J. (1990) *Biochemistry 29*, 2213−9.
53. Evans, C. T., Kurz, L. C., Remington, S. J., and Srere, P. A. (1996) *Biochemistry 35*, 10661−72.
54. Remington, S. J. (1992) *Curr. Opin. Struct. Biol. 2*, 730−5.
55. Monod, J., Wyman, J., and Changeux, J.-P. (1965) *J. Mol. Biol. 12*, 88−118.
56. Koshland, D. E., Jr., Nemethy, G., and Filmer, D. (1966) *Biochemistry 5*, 365−85.
57. Cornforth, J. W., Redmond, J. W., Eggerer, H., Buckel, W., and Gutschow, C. (1969) *Nature 221*, 1212−3.
58. Lenz, H., Buckel, W., Wunderwald, P., Biedermann, G., Buschmeier, V., Eggerer, H., Cornforth, J. W., Redmond, J. W., and Mallaby, R. (1971) *Eur. J. Biochem. 24*, 207−15.
59. Gerlt, J. A., and Gassman, P. G. (1993) *J. Am. Chem. Soc. 115*, 11552−68.
60. Lill, U., Lefrank, S., Henschen, A., and Eggerer, H. (1992) *Eur. J. Biochem. 208*, 459−66.
61. Kunkel, T. A., Roberts, J. D., and Zakour, R. A. (1987) *Methods Enzymol. 154*, 367−82.
62. Gandour, R. D., and Schowen, R. L. (1978) *Transition States of Biochemical Processes*, Plenum Press, New York.
63. Wilde, J., Lill, U., and Eggerer, H. (1990) *Biol. Chem. Hoppe-Seyler 371*, 707−13.
64. Albery, W. J., and Knowles, J. R. (1977) *Angew. Chem. Int. Ed. Engl. 16*, 285−93.
65. Sturtevant, J. M. (1977) *Proc. Natl. Acad. Sci. U.S.A. 74*, 2236−40.
66. Spolar, R. S., and Record, M. T., Jr. (1994) *Science 263*, 777−84.
67. Takahashi, K., Casey, J. L., and Sturtevant, J. M. (1981) *Biochemistry 20*, 4693−7.
68. Kurz, J. L., and Kurz, L. C. (1985) *Isr. J. Chem. 26*, 339−348.
69. Kohen, A., Cannio, R., Bartolucci, S., and Klinman, J. P. (1999) *Nature 399*, 496−9.
70. Johnson, J. K., and Srivastava, D. K. (1991) *Arch. Biochem. Biophys. 287*, 250−6.
71. Weidman, S. W., Drysdale, G. R., and Mildvan, A. S. (1973) *Biochemistry 12*, 1874−83.
72. Northrop, D. B. (1991) in *Enzyme Mechanism from Isotope Effects* (Cook, P. F., Ed.) pp 181−202, CRC Press, Boston.

BI991982R